The definitive version of this paper is published as:
Zangani, D.; Robinson, M.; Gibson, A.G. Evaluation of Stiffness Terms for Z-cored Sandwich Panels. *Applied Composite Materials* 2007, 14(3), 159-175.

Numerical and experimental validation of the stiffness terms of z-core sandwich panels

D. Zangani[a,*], M. Robinson[b] and A.G. Gibson[b]

[a]*D'Appolonia S.p.A., Via S. Nazaro, 19, 16145 Genova, Italy*
[b]*University of Newcastle upon Tyne, School of Mechanical & Systems Engineering, Stephenson Building, Newcastle upon Tyne, NE1 7RU, UK*

Abstract
This paper presents a model for the stiffness terms of z-cored composite sandwich panels (i.e. panels with truss-cores, corrugated-cores and double-corrugated cores containing a plastic foam). This model was validated, both through finite element simulation and comparison with the results of experimental three point tests on panels. A parametric study was performed to assess the performance of the different reinforced panel configurations.

Keywords: Sandwich composites, analytical modelling, Elasticity

1. Introduction

Sandwich panels are now widely used for lightweight structures because of their favourable strength-to-weight or stiffness-to-weight ratios. Modelling of simple sandwich panels can readily be accomplished using laminate theory [1] or sandwich theory [2] in simple cases, or finite element analysis (FEA) for more complex ones [3].

Recent processing developments have now rendered it possible to manufacture panels where the core is reinforced by means of trusses or corrugated structures connecting the skins: we will use the general term 'z-core' to describe structures of this type. Advantages of z-core panels can include improved strength, due to the suppression of skin debonding, as well as substantially improved impact performance. We present here a fairly straightforward numerical method of modelling and design of z-cored panels, the predictions of which will be compared with the results of simple bend tests and FEA predictions. The panel can be modelled as an equivalent homogeneous orthotropic thick plate, with appropriate elastic constants.

Several authors have provided models for the elastic constants of sandwich panels, including Libove and Hubka [4] and Fung and co-authors [5-6] who derived models for the elastic constants of panels with various types of load-bearing core. Collier, [7], derived the stiffness terms of stiffened composite panels using classical laminate theory (CLT) and modelled large stiffened panel structures with a single plane of shell finite 2D elements. Qiao and Wang [8] derived the elastic constants for panels with

* Corresponding author. Tel. +39 010 3628148; fax: +39 010 3621078.
E-mail address: donato.zangani@dappolonia.it (D. Zangani)

sinusoidal honeycomb cores and Lok and Cheng [9] studied truss-core sandwich panels, where the skin plates and the internal webs are fabricated using an extrusion process.

Z-core sandwich panels have been recently introduced in the railway and automotive areas [10].

2. Geometry of z-core panels

Figure 1 shows the core configurations considered in the present study. Figure 1a shows a single corrugated core panel. Figure 1b shows a double corrugated cored panel, which is sometimes a more suitable solution for thicker panels. Finally, Figure 1c shows a 'truss-core' configuration, which can be regarded as a particular case of the single corrugation. Here, here is desirable to enhance the bonding between the skin and the corrugation by stitching together or interweaving. Panels of this type can nowadays be conveniently fabricated by resin transfer moulding and related processes, which enable the required bonding to be achieved between the corrugation and the skins.

The main geometric parameters of a typical z-core sandwich panel, Figure 2, are:

- The contact breadth between the corrugation and the upper and lower face (W_{UF} and W_{LF});
- The thickness of the upper and lower face and of the corrugation (t_{UF}, t_{LF}, t_C);
- The corrugation angle (α).

In case of truss-core panels W_{UF} and W_{LF} are zero. The z-reinforced core can be designed to be stiff enough to make a significant contribution to the flexural rigidity in the *zx*-plane (*x* being the direction o f the corrugation and *z* the direction perpendicular to the plane of the panel). Consequently the usual sandwich panel assumption that the flexural rigidity of the core is negligible is no longer valid. A clear advantage of this configuration is that the risk of delamination between the core and the skins or sliding of the faces over one another is greatly reduced. If necessary the structure can be designed so that the webs of the corrugation sustain virtually all the shear load, reducing the contribution required from the foam and making possible the use of lower density, less expensive foam material.

3. Stiffness terms for z-core panels

The 'equivalent' properties of a z-cored panel can be found by a micromechanics approach, combined with laminate theory, as proposed by Collier [7], or through application of mechanics of material principles. The former approach enables equivalent in-plane and bending stiffnesses to be found, while the later also gives the longitudinal and transverse shear stiffnesses. Both approaches are considered in the present work.

Laminate theory assumptions include:

- the thickness of the lamina is much smaller than the in-plane dimensions;
- the strains in the deformed state are relatively are small;
- the vertical deflection does not vary through the thickness; and
- the stress normal to the plate surface is negligible.

Panel stiffness terms from laminate theory

The following model of the panel membrane, membrane-bending coupling, and bending stiffness terms is considered for single corrugated z-core panels:

$$\left(A_{ij}, -2B_{ij}, 3D_{ij}\right) = \sum_{k=1}^{n} \frac{\left((h_{k-1})^m - (h_k)^m\right)}{2p} \cdot \left(\overline{Q}_{ij}\right)_k \cdot \left[w_k \text{ or } \frac{t_k}{\sin\theta} \right] \qquad (1)$$

where:

[A] is the extensional stiffness matrix;
[B] is the membrane-bending coupling stiffness matrix;
[D] is the bending stiffness matrix;
$\overline{Q}$ is the transformed reduced layered elasticities of the laminae;
p is the corrugation pitch;
k is the identification subscript of layer or stiffening element
h is the height of the layer from the midplane of the panel (i.e. the reference plane)
m is the subscript for A, B, and D stiffness components (equal to 1,2 or 3) and
w, t, θ are the width, thickness, and angle of the stiffening element, respectively.

The presence of the corrugation oriented at an angle to the reference plane makes the panel structure heterogeneous. This can be modeled by dividing its thickness by the sine of the inclination angle. In this way each panel segment and its shape can be accounted for. The limitations of this approach are the same as those in lamination theory.

Equation (1) provides a mean of calculating the general stiffnesses and can be applied the three panel designs considered here. For the corrugated panel shown in Figure 2, the longitudinal stiffness terms (subscript 1,1) can be expressed as:

$$\left(A_{1,1}, -2B_{1,1}, 3D_{1,1}\right) = \left(\overline{Q}_{LF}\right)_{1,1} \cdot \left(h_1{}^m - h_0{}^m\right) + \frac{\left(\overline{Q}_C\right)_{1,1} \cdot \left(h_3{}^m - h_1{}^m\right)}{2p} w_{LF} + \frac{\left(\overline{Q}_C\right)_{1,1} \cdot \left(h_6{}^m - h_4{}^m\right)}{2p} w_{UF} +$$
$$+ \frac{\left(\overline{Q}_C\right)_{1,1} \cdot \left(h_5{}^m - h_2{}^m\right)}{p} \frac{t}{\sin\theta} + \frac{\left(\overline{Q}_F\right)_{1,1} \cdot \left(h_5{}^m - h_2{}^m\right)}{2p} \left(w_{UF} + w_{LF}\right) + \left(\overline{Q}_{UF}\right)_{1,1} \cdot \left(h_7{}^m - h_5{}^m\right)$$
(2)

Here the subscript, C, refers to indicates the corrugation, F, to the foam material, and LF and UF the lower and upper faces respectively.

Considering the stiffness perpendicular to the corrugation direction (i.e along the *y*-axis) and also the 12 coupling stiffness terms, it will be assumed that the contribution of the corrugation is limited to those segments that lie in the plane of the panel. This is because the 'accordion' shape of the corrugation renders it highly compliant in the transverse direction. For this case the stiffnesses are:

$$\left(A_{i,j},-2B_{i,j},3D_{i,j}\right)=\left(\overline{Q}_{LF}\right)_{i,j}\cdot\left(h_1{}^m-h_0{}^m\right)+\frac{\left(\overline{Q}_C\right)_{i,j}\cdot\left(h_3{}^m-h_1{}^m\right)}{2p}w_{LF}+\frac{\left(\overline{Q}_C\right)_{i,j}\cdot\left(h_6{}^m-h_4{}^m\right)}{2p}w_{UF}+$$
$$+\frac{\left(\overline{Q}_F\right)_{i,j}\cdot\left(h_5{}^m-h_2{}^m\right)}{2p}\left(w_{UF}+w_{LF}\right)+\left(\overline{Q}_{UF}\right)_{i,j}\cdot\left(h_7{}^m-h_5{}^m\right) \quad (3)$$

Here the contribution to the stiffness of the segment of the corrugation in the z-direction is removed. Similar expressions to Equations (2) and (3) can be obtained for the double corrugated and truss core sandwich configurations of Figure 1b and 1c. These calculated panel stiffnesses can now be used in FEA of structures with shell elements having 'smeared' properties equivalent to the panel properties.

In-plane engineering constants

Equation (1) provides the stiffness terms of the panel calculated as the summation of all layers or stiffening element contributions. When the necessary initial data are available, the analysis provides the engineering constants that define the constitutive behaviour of the panel, evaluated using the analogy between the ply compliance and the normalised in-plane compliance matrices. As in the case of a laminated composite plate the equivalent engineering constants can be calculated as follows:

$$E_x=\frac{1}{h\cdot a_{11}};\ E_y=\frac{1}{h\cdot a_{22}};\ G_{xy}=\frac{1}{h\cdot a_{33}} \quad (4)$$

and the Poisson's Ratios are:

$$\nu_{xy}=-\frac{a_{12}}{a_{11}};\ \nu_{yx}=-\frac{a_{12}}{a_{22}} \quad (5)$$

Here h is the distance between the centerline of the upper and lower skin and the a_{ij} terms are the components of the compliance matrix.

Extensional Stiffnesses

As an alternative to Equation (4), considering symmetrical sandwiches, the extensional stiffnesses of a corrugated core panel can also be obtained from the relationship between the force and the corresponding deformation in the longitudinal and transverse direction (*x*- and *y*-direction respectively), giving the following:

$$E_x=\overline{EA}_x \quad (6)$$

$$E_y=\frac{\overline{EA}_y}{1-\nu_1{}^2\cdot\left(1-\frac{\overline{EA}_y}{\overline{EA}_x}\right)} \quad (7)$$

where

$\overline{EA}_x = E_C \bar{A}_C + 2 \cdot E_1 \cdot t_1$

$\overline{EA}_y = 2 \cdot E_1 \cdot t_1$

EC modulus of elasticity of core material

$\bar{A}_C$ area, per unit width, of corrugation cross section perpendicular to corrugation axis

E1 modulus of elasticity of the upper and lower skin

t1 skin thickness

ν1 Poisson's ratio of the skin material

The above expressions are derived on the assumption that the moment, M_x, and force, F_x, are resisted by both the bending and extensional stiffnesses of the corrugation and the extensional stiffnesses of the upper and lower skins. The moment, My, and the force, Ny, are assumed to be resisted only by the extensional stiffnesses of the skins.

The Poisson ratios associated with extension are given by:

$$\nu_{xy} = \nu_1 \text{; and } \nu_{yx} = \nu_{xy} \cdot \frac{E_y}{E_x} \tag{8}$$

Bending Stiffness

The bending stiffnesses are obtained from the following expressions:

$$D_x = \overline{EI}_x \tag{9}$$

$$D_y = \frac{\overline{EI}_y}{1 - \nu_1^2 \cdot \left(1 - \frac{\overline{EI}_y}{\overline{EI}_x}\right)} \tag{10}$$

where

$\overline{EI}_x = E_C \bar{I}_C + \frac{1}{2} \cdot E_1 \cdot t \cdot h^2 + \frac{1}{2} \cdot E_C \cdot t_C \cdot h_C^2 \cdot \left(\frac{w_{UF} + w_{LF}}{2p}\right)$

$\overline{EI}_y = \frac{1}{2} \cdot E_1 \cdot t \cdot h^2$

where $\bar{I}_C$ is the moment of inertia, per unit width, of corrugation cross section area about the mid-plane and t is the skin thickness (assumed to be the same for both skins in this case).

Transverse shear stiffness

In deriving the transverse shear stiffness in planes parallel to the corrugation, we need to consider an element of the z-core sandwich of length, dx, and width, 2p, under a transverse shear, D_x. The transverse shear is equilibrated by the variation of bending moment dM along the element.

Assuming the only flexibility of the above element to be that of the corrugation in shear, the transverse shear stiffness can then be expressed as:

$$D_{Q_x} = \frac{Q_x}{\gamma_x} = G_C \cdot t_c \cdot \frac{I \cdot h}{p \cdot \int_0^l Q\,ds} \tag{11}$$

where:

γ_x the angle representing the average shear strain, equal to $\delta x/h$
I is the moment of inertia of width 2p of cross section parallel to yz-plane
p is the corrugation pitch
l is the length of one corrugation leg measured along the center line
Q is the static moment about the middle plane of the sandwich

When in-plane isotropic material is used for the skin and corrugations, Equation (11) becomes [9]:

$$D_{Q_x} = G_C \cdot t_c \cdot \frac{\frac{h^2 \cdot t}{p \cdot 2d \cdot t_c} + \frac{1}{6} \cdot \left(\frac{h_c}{p}\right)^2}{\frac{t}{t_c} + \frac{2d \cdot h_c}{3ph}} \tag{12}$$

This can be further simplified if only the skin contribution to bending stiffness is considered, which leads to constant shear flow in the corrugation, and the following approximation:

$$D_{Q_x} = \frac{G_C \cdot t_c^{\,2}}{\overline{A}_c} \cdot \left(\frac{h}{p}\right)^2 \tag{13}$$

where $\overline{A}_c$ is the corrugation cross-sectional area per unit width, and t_c is the corrugation thickness.

The transverse shear stiffness in planes perpendicular to the corrugation axis is obtained considering an element of the sandwich having unit width in the direction normal to the page and in equilibrium under a small transverse shear of unit intensity (Qy=1) and horizontal forces Y of intensity p/h. As described in [9] for a truss-core sandwich panel, the transverse shear stiffness, D_{Q_y}, is given by the ratio of the shear intensity to shear strain, or:

$$D_{Q_y} = \frac{1}{\gamma_y} = \frac{1}{\frac{\delta_y}{h} - \frac{\delta_z}{p}} \tag{14}$$

The sandwich can then be treated as a statistically indeterminate structure to determine the displacements δ_y and δ_z. Substituted these into Equation (14) gives the following expression for transverse shear stiffness:

$$D_{Q_y} = C \cdot h \cdot \left(\frac{E_c}{1-\nu_c^{\,2}} \right) \cdot \left(\frac{t_c}{h_c} \right)^2 \tag{15}$$

where C is a non-dimensional coefficient depending upon the shape of the corrugation. For the case of symmetrical corrugated core sandwiches (as in Figure 1), the coefficient, C, obtained from the general expression of Libove and Hubka [4] is:

$$C = \frac{6\frac{h_c}{p}C_1C_4 + \left(\frac{p}{h_c}\right)^2}{12\left\{-2\left(\frac{p}{h_c}\right)^2 C_2 + \frac{h_c}{h_p}\left[6C_4\left(C_1C_3 - C_2^{\,2}\right) + \left(\frac{p}{h_c}\right)^3 C_3\right] + \frac{h_p}{h_c}\frac{p}{h_c}C_1\right\}} \tag{16}$$

where:

$$C_1 = K_{I_Z} + \frac{1}{12}\frac{E_c}{E'_c}\left(\frac{t_c}{h_c}\right)^2 \sin\theta$$

$$C_2 = K_{I_{YZ}} - \frac{1}{12}\frac{E_c}{E'_c}\left(\frac{t_c}{h_c}\right)^2 \sin\theta\cos\theta$$

$$C_3 = K_{I_Y} + \frac{1}{12}\frac{E_c}{E'_c}\left(\frac{t_c}{h_c}\right)^2 \left(\frac{W}{h_c} + 2\frac{d}{h_c}\cos\theta\right)$$

$$C_4 = \frac{E_1}{E_c}\frac{1-\nu_c^{\,2}}{1-\nu_1^{\,2}}\left(\frac{t_1}{t_c}\right)^3 \tag{17}$$

$$K_{I_Z} = \frac{1}{h_c^{\,3}}\int y^2 ds = \frac{2}{3}\left(\frac{d\cdot\cos\theta}{h_c}\right)^2 \frac{d}{h_c} + \frac{2}{3}\left[\frac{1}{8}\left(\frac{p}{h_c}\right)^3 - \left(\frac{d\cdot\cos\theta}{h_c}\right)^3\right]$$

$$K_{I_{YZ}} = \frac{1}{h_c^{\,3}}\int yz\, ds = \frac{1}{3}\frac{d^2\cdot\cos\theta}{h_c^{\,2}} + \frac{1}{2}\left[\frac{1}{4}\left(\frac{p}{h_c}\right)^2 - \left(\frac{d\cdot\cos\theta}{h_c}\right)^2\right]$$

$$K_{I_Y} = \frac{1}{h_c^{\,3}}\int z^2\, ds = \frac{1}{6}\frac{d}{h_c} + \frac{1}{4}\frac{W}{h_c}$$

E_c and E'_c are the bending and extensional modulus of the corrugation, respectively. The main simplification with respect to the general expression of the non-dimensional coefficient at the basis of Equation 17 is that the radius of curvature of the corrugation sheet between the contact area with the skins and the internal core is assumed to be zero. This is compatible with structures where the corrugation is made from reinforcements that are highly conformable.

For truss-core sandwich (Figure 1c) D_{Qy} is obtained by considering the length of the contact segment between the corrugation and the skins, W, to be zero. For a double

corrugated core sandwich (Figure 1b) D_{Qy} can be obtained from the model for single corrugated core with upper and lower skin thickness equal to zero.

4. Experimental and FE validation

Validation of the analytical expressions was achieved by comparing the stiffness terms of the reinforced sandwich panels calculated using the proposed models with both the results of 3D FEA and with experimental results. The benchmark for the validation of the analytical models of the panel stiffness terms is given by the three-point bending test on corrugated sandwich panels, performed within the research project Hycotrans by the University of Perugia and described in detail elsewhere [11]. The test specimens had a width of 140 mm and length of 300 mm. This ensured that the samples were wide enough to contain a representative section of the internal panel structure. The two facings were made by three layers of 1168 g/m^2 $[0/45/90/45]_s$ non-crimp quadriaxial E-glass mat; the corrugation was formed from two layers of the same reinforcement, placed back-to-.back to produce a symmetric laminate. The matrix was a phenolic liquid resin (J2027L supplied by Blagden Chemicals, Sully, UK). This was cured using a general purpose sulphonic acid catalyst, also supplied by Blagden Chemicals. The foam was a phenolic foam (Contratherm C70-130) provided by Alderley Materials (Berkeley, UK). The resulting thickness of the facings was 2.7 millimetres, with a standard deviation of 0.38 mm. The overall thickness of the panel was in average 35 millimetres with a standard deviation of 1.90 mm. Relevant properties of all the components used in the panels are given in Table 1.

Laminates were tested in accordance with ASTM C 393-94, the results again being summarised in Table 1. The fibre weight fraction was 63%, corresponding to a fibre volume fraction of 43%. The same value was assumed for the longitudinal and transverse modulus for the laminate.

5. Results

To highlight any asymmetry effects in the case of the single corrugation panels the 3-point bend tests were carried out with samples in both possible configurations. Figure 4 shows the load deflection curve of the panels in the ‘narrow side up’ configuration, as sketched, and Figure 5 shows the results in the inverted configuration. The maximum loads and, the shape of the curve are similar in both cases: the load grows almost linearly up to a maximum value of the load, the peak load, and then it decreases to a value of about 0,70-0,75 of the peak load. It was also observed that the shape of the curve would suggest the failure of the structure was due to instability. As shown in the next paragraph, the numerical analyses have demonstrated this hypothesis was correct.

6. Numerical Validation

FEA modelling was carried with three-dimensional models representative of the specimens tested. The purpose of the bending modelling was to validate the numerical model by comparison with the experimental results and, in turns, to validate the stiffness terms obtained with the analytical models. For the validation of the stiffness terms, the linear portion of the force-displacement curve is of interest. However also the understanding of the behaviour of the panel in the non-linear region of the curve and

the failure behaviour of the panel is of interest for the optimal use of the panel configuration with corrugated core. The FE analysis of the bending test is therefore extended to the non-linear part of the force-deformation curve, in a region where large displacements need to be included in the model.

In order to reduce the number of degrees of freedom of the model it has been taken advantage of the symmetry conditions and of the repetitive geometrical patterns in the structure. The finite element representation used in this study is a one-quarter symmetric model. The FE model employed a panel length of 475 mm, a width of 140 mm and a thickness of 33 mm. Shell element type SHELL91 and solid element type SOLID95 were used from the ANSYS library. SHELL91 has six degrees of freedom at each node: translations in the nodal x, y, and z directions and rotations about the nodal x, y, and z axes. SOLID95 is defined by 20 nodes having three degrees of freedom per node: translations in the nodal x, y, and z directions. The shell elements were used for the modelling of the composite facings and the internal corrugation. It was exploited the possibility offered by the shell element used to define the properties of each layer in the composite laminate, even if the reinforcement used is actually characterised by in-plane isotropic properties. In this way the actual laminate staking sequence could have been defined. The internal foam in between the composite layers has been modelled using volume elements. The finite element nodes for each element in the model, including those corresponding to the facings, the corrugation, and the foam, are coincident with the nodes of the adjacent element.

The nodes in correspondence of the lateral supports were constrained to the vertical displacements. The progressive loading of the specimen in the mid section was simulated by applied vertical displacements to the upper nodes of the panel with increasing value, from 1 millimetre up to a value of 50 millimetres applied displacement with 1 millimetre step. Both the “top” and “bottom” configurations were modelled in order to detect any difference in the behaviour of the structure, in particular in correspondence of the non-linear portion of the force/displacement curve. The two models are equivalent apart for the selection of the nodes which are constrained to simulate the supports and the nodes where the displacements are applied.

The foam elements were included in the simulations up to a certain value of the applied displacement, of about 15 millimetres, in correspondence of the decreasing portion of the load-displacement curve. After such value of applied displacement, the volume elements of the foam were removed from the model because of the excessive distortions of the elements in some regions of the model. Without the foam elements it was be possible to carry out the simulations up to a value of applied displacements of 50 millimetres, almost the same value of the maximum displacement applied in the experimental tests. As shown in Figure 4, and Figure 5 the results of the bending modelling are in good agreement with the experimental test curves. The simulation of the bending test of the panels in the ‘narrow side up’ configuration (“top” configuration”) slightly underpredicts the value of the maximum bending force and of the residual force in the plateau region of the curve, while in the inverted configuration, shown in Figure 4, a better agreement is achieved, with only a minimum shift of the value of the displacement corresponding to the maximum load. This difference is explained by the presence within the sample of additional material not included in the

model, in particular resin rich areas localised in the region between the corrugation and the upper facing. Such material is compressed when bending the sandwich in the narrow up configuration, making a contribution to the overall resistance which could be not taken into account in the simulations. In any case, the agreement of the experimental curves with the simulation is excellent and within the usual levels of acceptance in the engineering practice. Interesting is the analysis of the deformed configurations which are shown in Figure 6. The simulation allows confirming the hypothesis of failure due to local instability. In case of the top configuration, the load applied in the centre of the specimen causes the corrugation sheets to buckle towards the lateral faces of the sandwich, with rotation of the connection between the facings and the web of the corrugation and subsequent distortion of the cross section, with the lower facing bending upward to follow the deformation of the corrugation. In case of the "bottom" configuration, the corrugation webs buckle inwards compressing the foam internal to the sandwich, and forcing the lower facing to bend downward.

The failure mechanism of the panel is therefore governed by the local instability of the corrugation webs, and a stable post-buckling response corresponding to the force plateau observed in the experimental tests. A more detailed description of the numerical simulations will be included in a future paper dealing with the failure behaviour of the z-core sandwich structures and the stability of the web elements. For the purpose of the validation of the analytical expressions of the stiffness terms of the panel the availability of a validated numerical model in the elastic regime was required. The following step is the determination of the flexural and shear rigidities by analysing the deflection of the panel subjected to a three point load test. The deflection Δ under a point load W is given by:

$$\Delta = \Delta_1 + \Delta_2 = \frac{WL^3}{48D} + \frac{WL}{4AG} \tag{18}$$

where D is the flexural rigidity, AG is the shear stiffness of the sandwich and L is the span.

The above equation can be reformulated in two ways:

$$\frac{\Delta}{WL} = \frac{L^2}{48D} + \frac{1}{4AG}$$

$$\frac{\Delta}{WL^3} = \frac{1}{48D} + \frac{1}{4AG} \cdot \frac{1}{L^2} \tag{19}$$

The first of the above equations can be represented as a straight line in a plot of Δ/WL against L^2, the second as a straight line in a plot of Δ/WL^3 against $1/L^2$. From the value of the slope of the line in the first graph it is possible to estimate the bending stiffness D, while from the intercept it is possible to obtain an approximate value of the shear stiffness AG. The opposite from the value of the slope and of the intercept form the second graph. If the flexibility Δ/W of the panel is measured at a number of different spans, the required stiffnesses D and AG may be obtained from the slopes and the

intercepts on the vertical axes of the two graphs [12]. In the current study, only the results of experimental tests on a single span length (275 millimetres) were available, as described in previous Paragraph 5. The approach chosen for the calculation of the bending and shear stiffness was the following: the actual test conditions were considered in a FE calculation in order to validate the numerical model. Another calculation was developed considering a different value of the span length (375 millimetres) than that one of the experiments in order to obtain the second point required to draw the line required to obtain the straight lines in the above graphs. The comparison of the values of the stiffness terms calculated using the analytical expressions and the values resulting from the numerical modelling and the experimental results is reported in next Table 2. Very good agreement was achieved between the analytical and the numerical/experimental results.

7. Comparisons of panel configurations

A comparison of the performance of the three panel configurations (simple corrugation, double corrugation and truss-core) was carried out, based on a 'performance index' defined as follows [13]:

$$I_p = \frac{D_i^{corrugated} \Big/ \left(A_{corrugated}\right)^2}{D_i^{unre\,inf\,orced} \Big/ \left(A_{facings}\right)^2} \tag{20}$$

where $D_i^{corrugated}$, is the equivalent stiffness of the z-core sandwich panel (for example D_x, D_y, or D_{Qx}), $D_i^{unre\,inf\,orced}$ is the equivalent stiffness of a sandwich panel of similar geometry but without the internal reinforcement, $A_{corrugated}$ is the area of the composite material (skin and corrugation) in the section, A_{skins} is the area of the composite skins only of the unreinforced sandwich used as a reference.

The parameter, I_p, can be used as an indicator of the performance of a particular design. The variation of I_p was examined for different values of the ratio h/2p (the panel thickness divided by the corrugation pitch). Four values of h/2p were considered: 0.25, 0.40, 0.60 and 1.00. Tables 3 and 4 show the dimensions and details of the configurations studied. Figures 7 and 8 show the performance index, I_p, of the three panel configurations in terms of equivalent extensional stiffness along the longitudinal, E_x, and transverse direction, E_y, respectively. In the case of the extensional longitudinal stiffness it can be observed that all the three configurations behave similarly, with a lower index than that of an equivalent unreinforced sandwich panel. This is mainly due to the higher value of the composite area of the section.

In the case of the transverse direction extensional stiffness the internal reinforcement does not make any contribution and therefore the performance are of the order of 50% than an unreinforced sandwich panel. This underlines the importance when using a reinforced panel to orient it along the direction of the maximum stress.

The performance index of the reinforced panels with respect to longitudinal bending stiffness, D_x, and transverse bending stiffness D_y, is shown in Figure 9 and Figure 10,

respectively. Simple and double corrugated panels show better bending properties than the truss configuration, mainly due to the contribution of the corrugation segment in contact with the upper and lower skins. The truss core panel shows the lowest bending stiffness, due to the limited contribution of the webs.

All the comparisons, based on elastic behaviour of the panels, show z-cored panels to be inferior to simple sandwiches. This is not surprising, given that the simple sandwich is the most effective configuration considering only stiffness to weight. However, as stated above, the advantages come in improved failure loads and failure modes as well as in better performance in energy absorption.

8. Conclusions

The use of equivalent stiffness terms allows the modelling of sandwich structures with internal reinforcement as equivalent orthotropic thick plates. The model solutions compare well with both the experimental test results and with the results of FE modelling.

A parametric study has been carried out to compare the performance of different panel configurations. The model presented here has the potential to be used to develop tools for optimal design and fast analysis of structures made with z-core reinforced sandwich panels.

Acknowledgements

This work was supported by the European Commission under the GROWTH Project "Hybrid Composite Production for the Transportation Sector, HYCOPROD", Contract Number G3RD-CT-1999-00060.

REFERENCES

1 Halpin J. C., 1984, “Primer on Composite Materials: Analysis”, Technomic Publishing.

2 Allen H.G., 1969, “Analysis and Design of Structural Sandwich Panels”, Pergamon Press

3 Ha KH., 1991, “Finite Element Analysis of Sandwich Construction: a Critical Review”, Sandwich Constructions

4 Libove, C., Hubka R.E., 1951, “Elastic Constants for corrugated-core sandwich plates”, Internal Report, NACA TN 1526

5 Fung T.C., K.H. Tan, T.S. Lok, 1994, “Elastic Constants for Z-core Sandwich Panels”, Journal of Structural Engineering, Vol. 120, No. 10, October

6 Fung T.C., K.H. Tan, T.S. Lok, 1996, “Shear Stiffness D_{Qy} for C-Core Sandwich Panels”, Journal of Structural Engineering, Vol. 122, No. 8, August

7 Collier C.S., 1993, “Stiffness, Thermal Expansion, and Thermal Bending Model of Stiffened, Fiber Reinforced Composite Panels”, AIAA/ASME/ASCE/AHS/ACS 34th Structures, Dynamics, & Materials Conference

8 Qiao P., J. Wang, 2005, “Mechanics of Composite Sinusoidal Honeycomb Cores”, Journal of Aerospace Engineering, Vol. 18, No. 1, January

9 Lok Tat-Seng, Cheng Quian-Hua, 2000, “Elastic Stiffness Properties and Behaviour of Truss-Core Sandwich Panel”, Journal of Structural Engineering, Vol. 126, No. 5, May.

10 Robinson M., “Application in Trains and Railways”, *Comprehensive Composite Materials*, Volume 6: Design and Applications, Elsevier, 2000.

11 Zangani D., A. Barbagelata, O. Manni, G. Mastrobuono, "Modelling of Composites for Rail Vehicles", *Composites in the Rail Industry II Conference*, Birmingham, 28 October, 1999.

12 Nordstrand T.M., L. A. Carlsson, 1997, “Evaluation of transverse shear stiffness of structural core sandwich plates”, Composite Structures No. 37

13 Ashby M.F., 1992, “Materials Selection in Mechanical Design”, Pergamon Press

Table 1
Properties of individual sandwich panel constituents and laminate.
E-glass fibre, cast Cellobond phenolic, C70-130 foam and laminate.

	E-glass fibre	Phenolic resin	C70-130 foam	Skin and corrugation laminate
Density ($kg.m^{-3}$)	2560	1100	130	
Young's Modulus (GPa)	76	3.4	0.026	15.4
Shear modulus (GPa)	—	—	—	5.5
Tensile strength (MPa)	2100	32	—	198
Compressive strength (MPa)	—	—	0.91	218
Shear strength	—	—	0.80	139
Poisson's ratio	0.22	0.32	0.34	0.16
Tensile failure strain (%)	2.6	1.5	—	—

Table 2
Comparison of bending stiffness values

Properties	$\mathbf{D_x}$	$\mathbf{D_{Qx}}$
	N·mm	$N \cdot mm^{-1}$
Analytical	$4.51 \cdot 10^6$	$2.531 \cdot 10^3$
Numerical/Experimental	$4.48 \cdot 10^6$	$2.48 \cdot 10^3$

Table 3
Geometric parameters of the z-core sandwich panel configurations studied

	h/S	**2p** (mm)	**H** (mm)	**t_c** (mm)	**W** (mm)	**t** (mm)	**h_c** (mm)	**θ**
Simple corrugation	0.25	140	34.5	2.0	41.5	2.5	27.5	44.0
	0.40	100	40	2.5	30	5.0	27.5	54.0
	0.60	100	60	2.5	30	5.0	47.5	67.2
	1.00	50	50	2.5	10	5.0	37.5	68.2
Double corrugation	0.25	140	34.5	2.0	55.75	2.5	12.75	41.8
	0.40	100	40	2.5	30	5.0	12.5	32.0
	0.60	100	60	2.5	30	5.0	22.5	48.4
	1.00	50	50	2.5	10	5.0	17.5	49.4
Truss core	0.25	35	34.5	2.0	0	2.5	27.5	57.5
	0.40	50	40	2.5	0	5.0	27.5	47.7
	0.60	50	60	2.5	0	5.0	47.5	62.2
	1.00	50	50	2.5	0	5.0	37.5	56.3

Table 4
z-core sandwich panel configurations studied

	Simple Corrugation	Double Corrugation	Truss-Core
h/2p=0.25			
h/2p=0.40	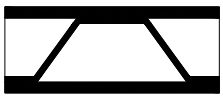	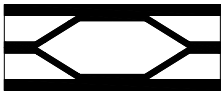	
h/2p=0.60	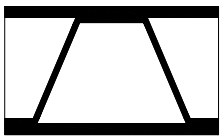	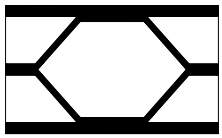	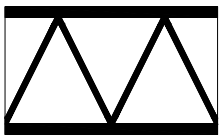
h/2p=1.00		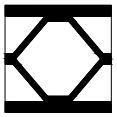	

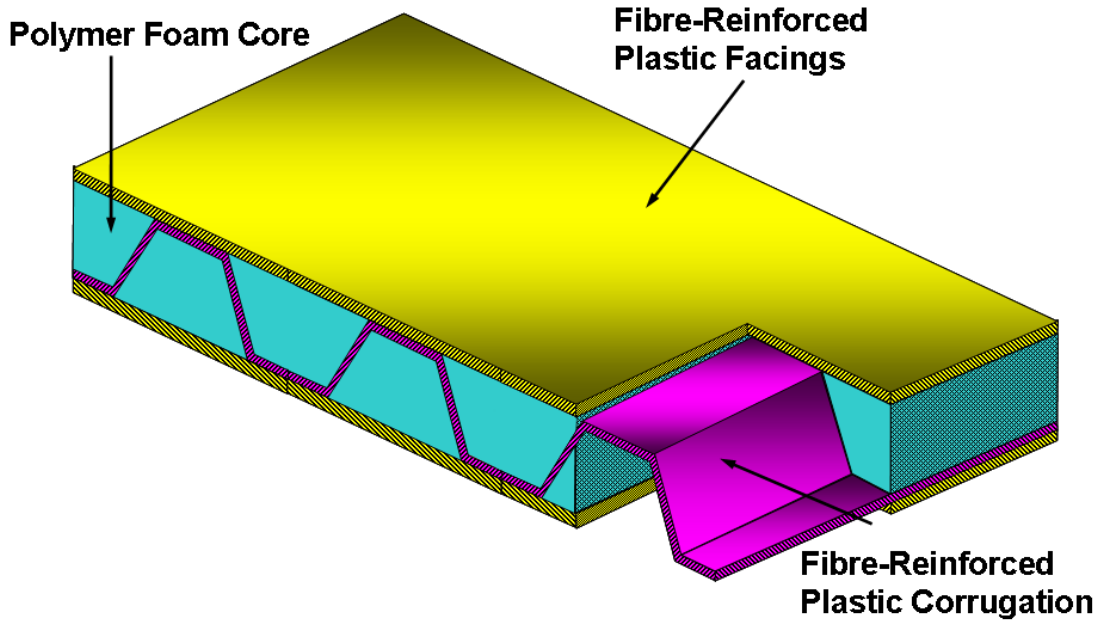

(a) Single corrugation

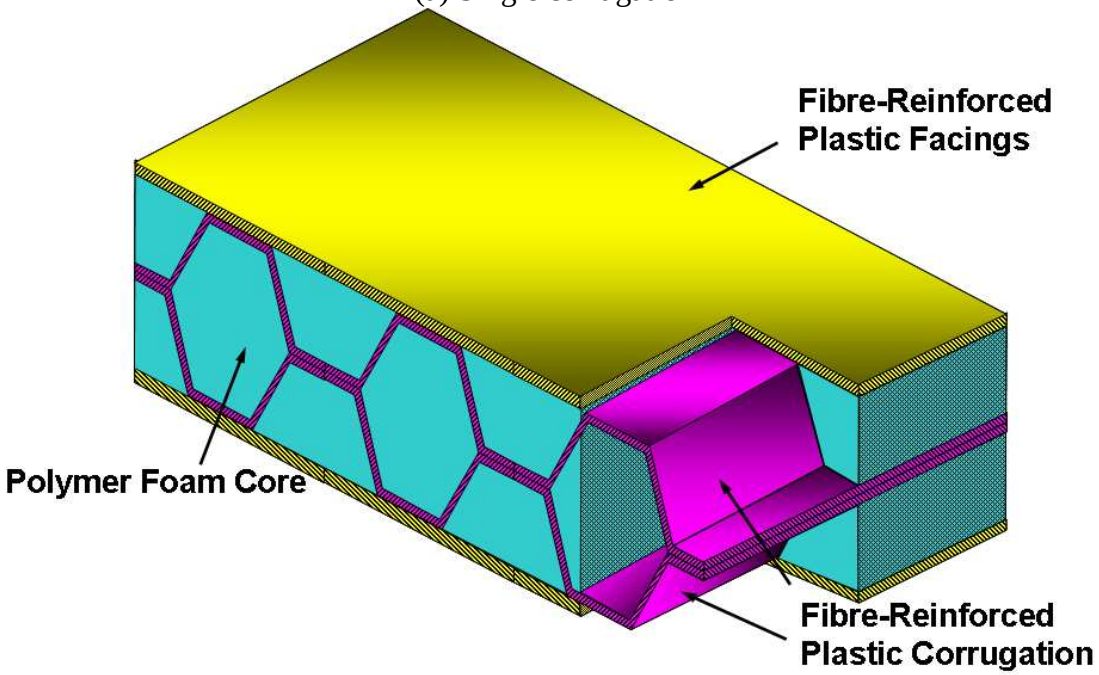

(b) Double corrugation

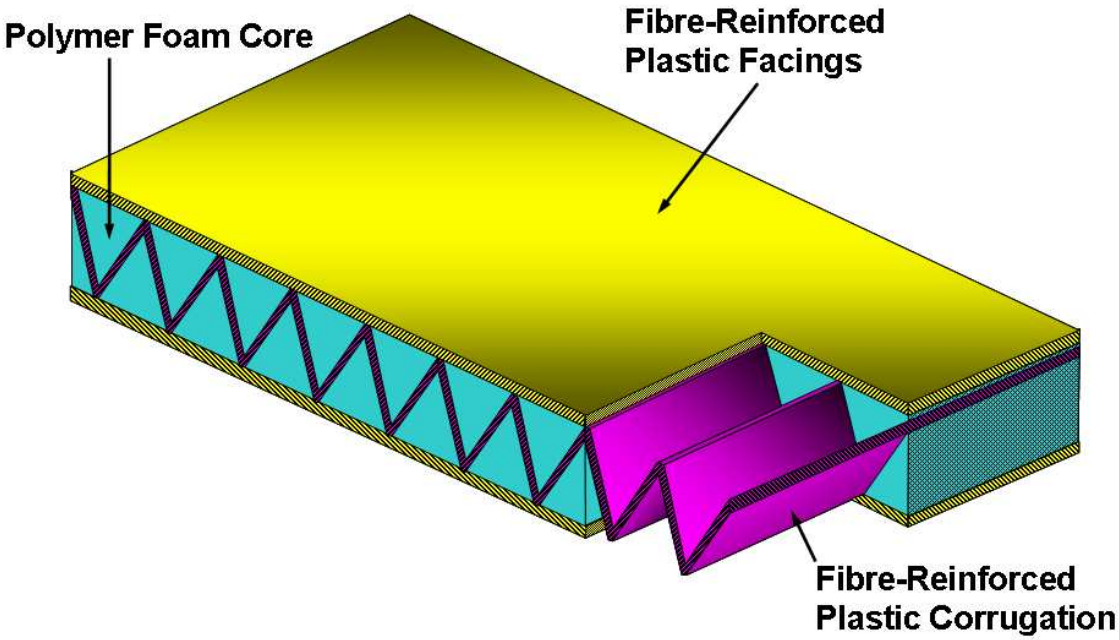

(c) Truss-core

Figure 1. z-core sandwich panel configurations. (a) single corrugation core, (b) double corrugation core, and (c) truss-core.

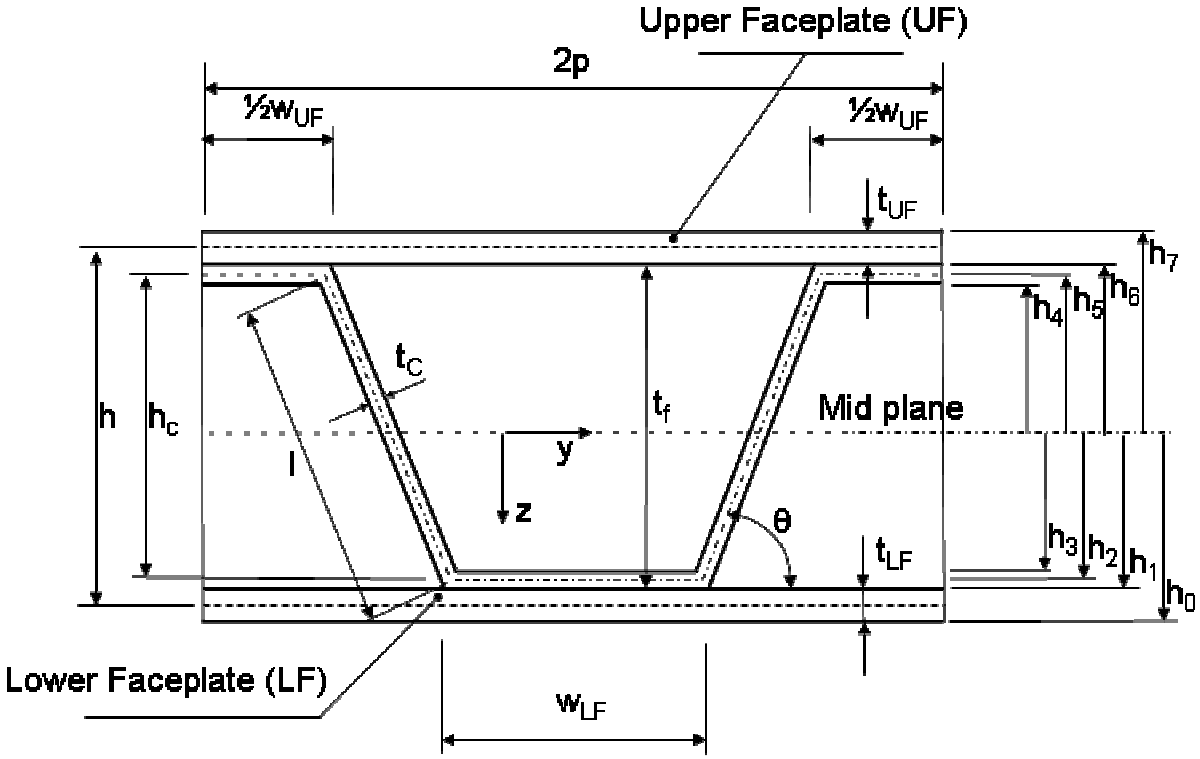

Figure 2. Geometrical parameters defining the z-core sandwich panel geometry.

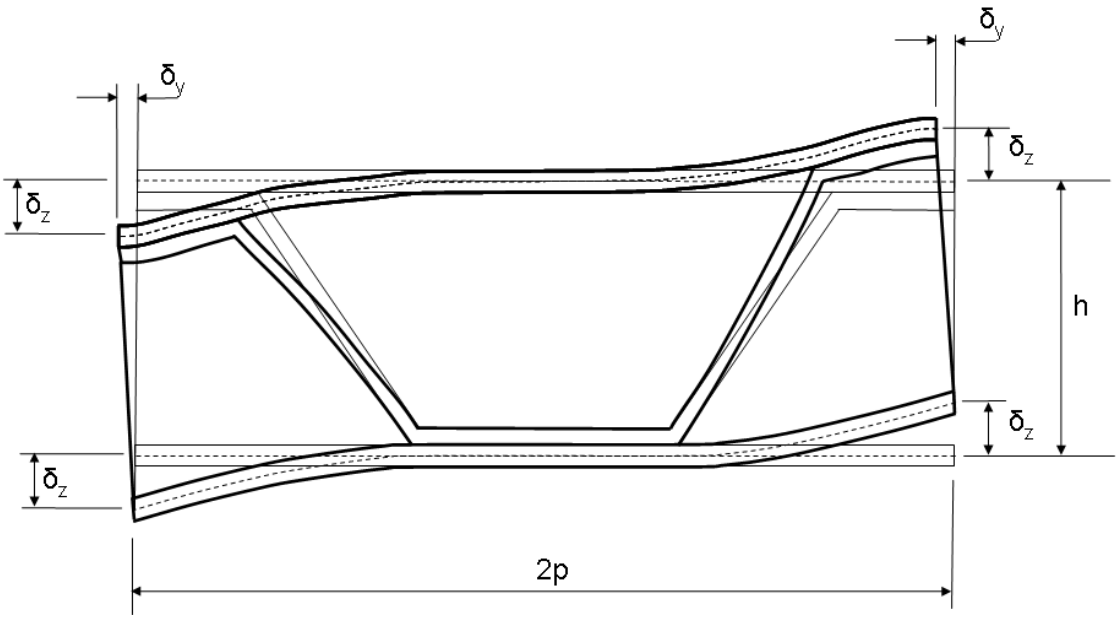

Figure 3. Deformation of a corrugated z-core sandwich panel subjected to transverse shear in planes perpendicular to the corrugation.

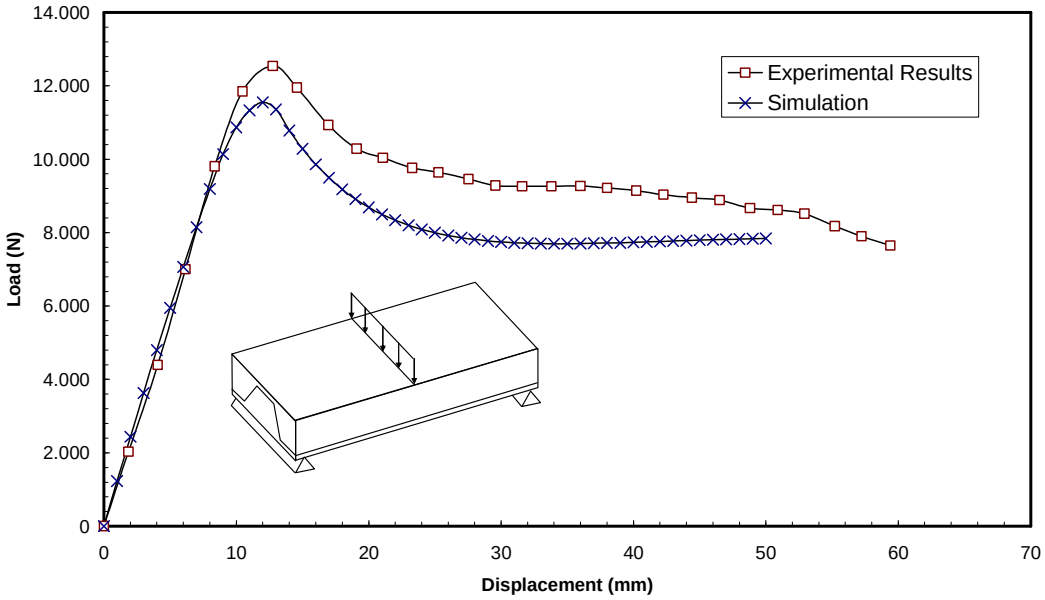

Figure 4. 3-point bending tests: load-deflection curve for corrugated core sandwich panels with the core in the 'narrow side up' or 'top' configuration. Comparison between experiments and simulation

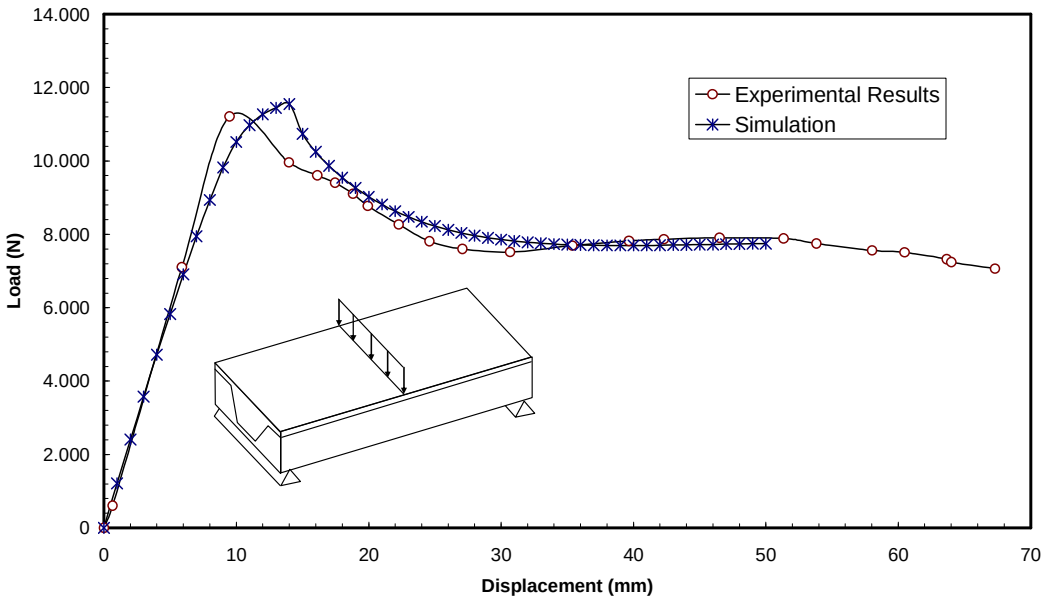

Figure 5. 3-point bending tests: Load-deflection curve for corrugated core sandwich panels in the ‘narrow side down’ or ‘bottom’ configuration. Comparison between experiments and simulation

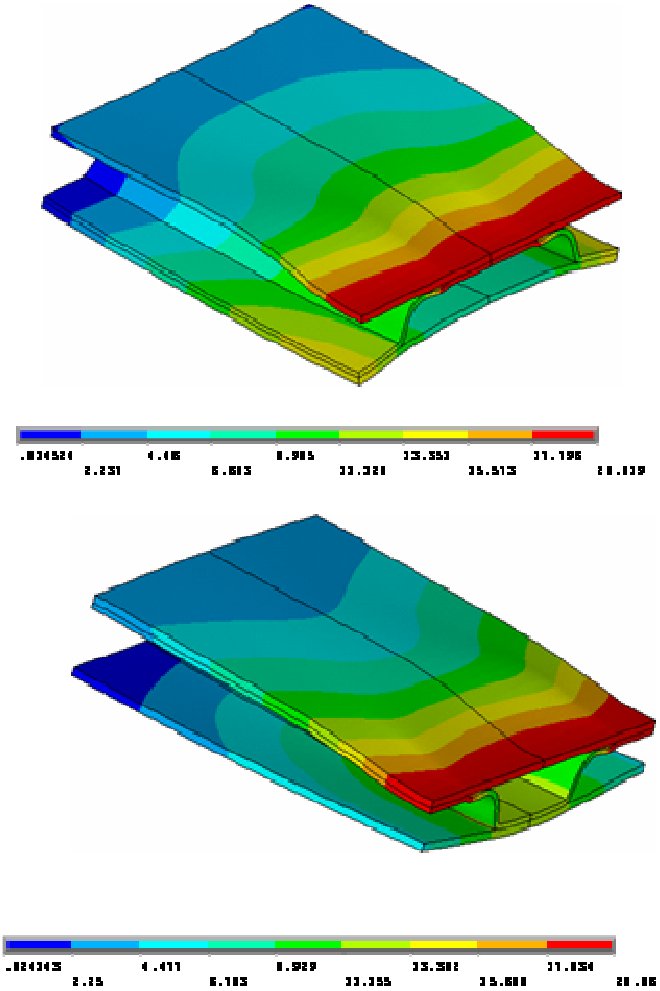

Figure 6. Deformation of the composite layers in the panel during the bending test, Top configuration (left and Bottom configuration (right) (millimetres).

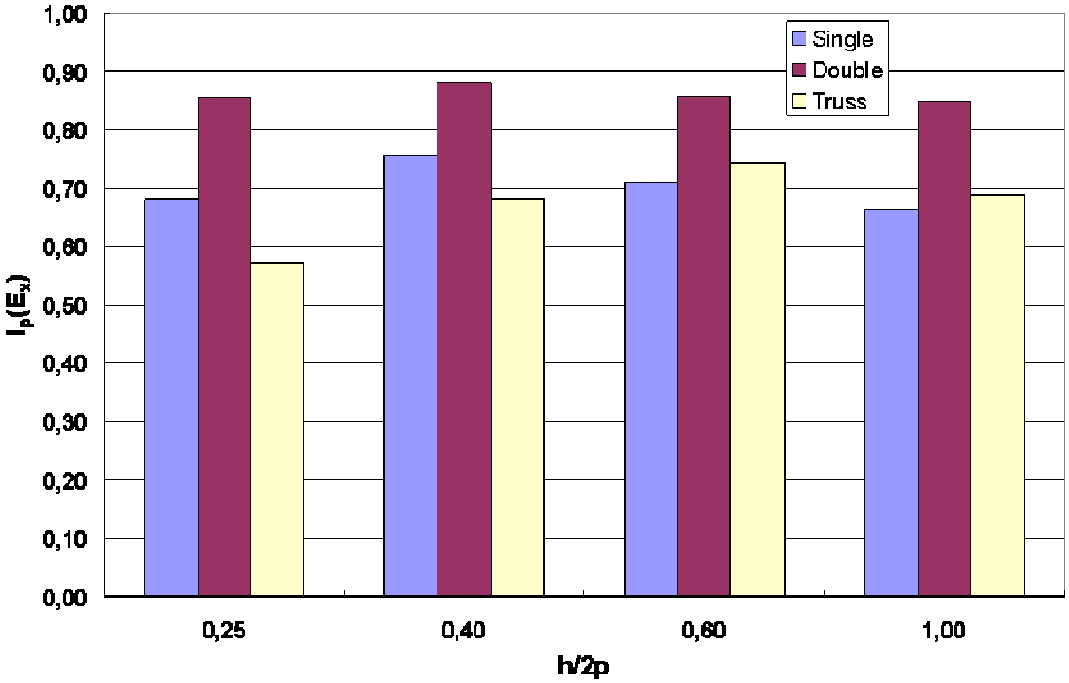

Figure 7. Performance of the sandwich configurations with respect to equivalent Ex.

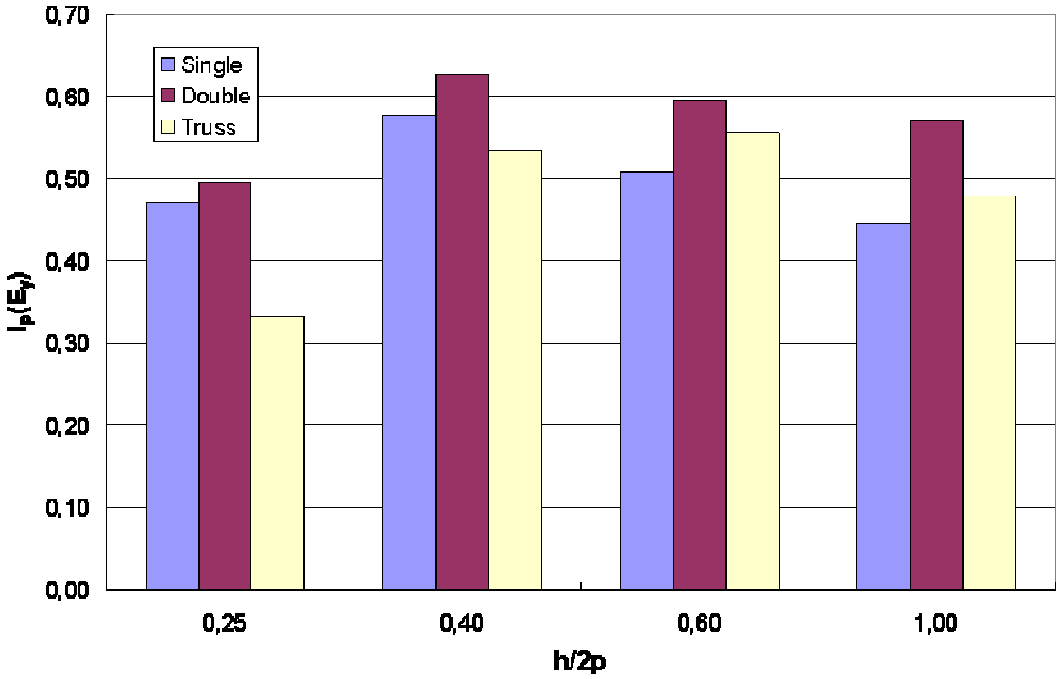

Figure 8. Performance of the sandwich configurations with respect to equivalent Ey.

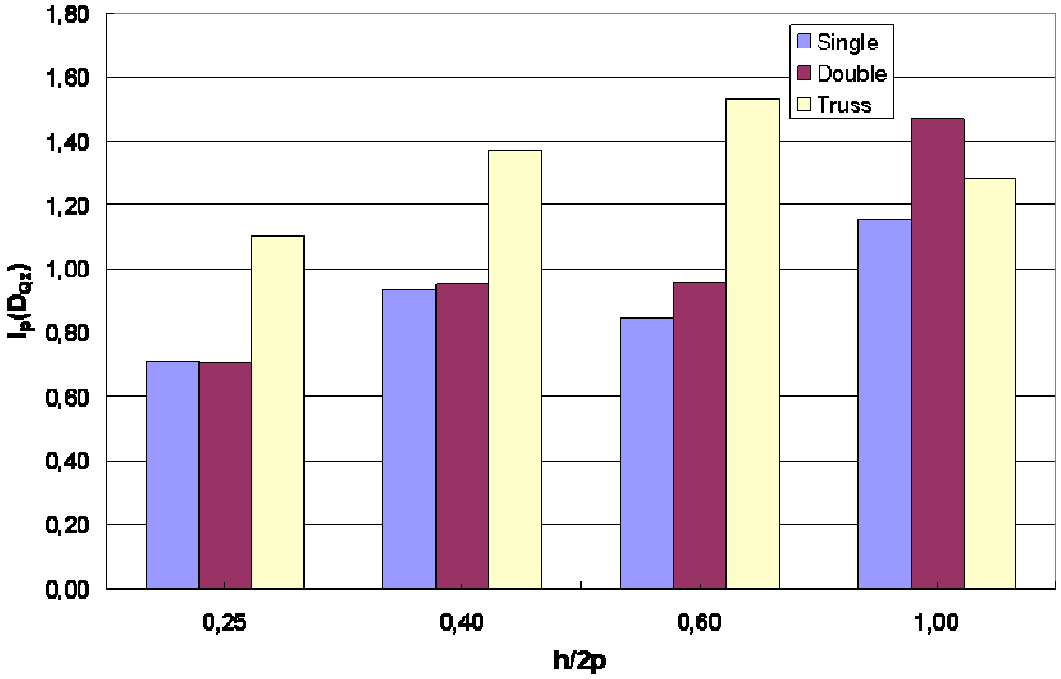

Figure 9. Performance of the sandwich configurations with respect to equivalent Dx.

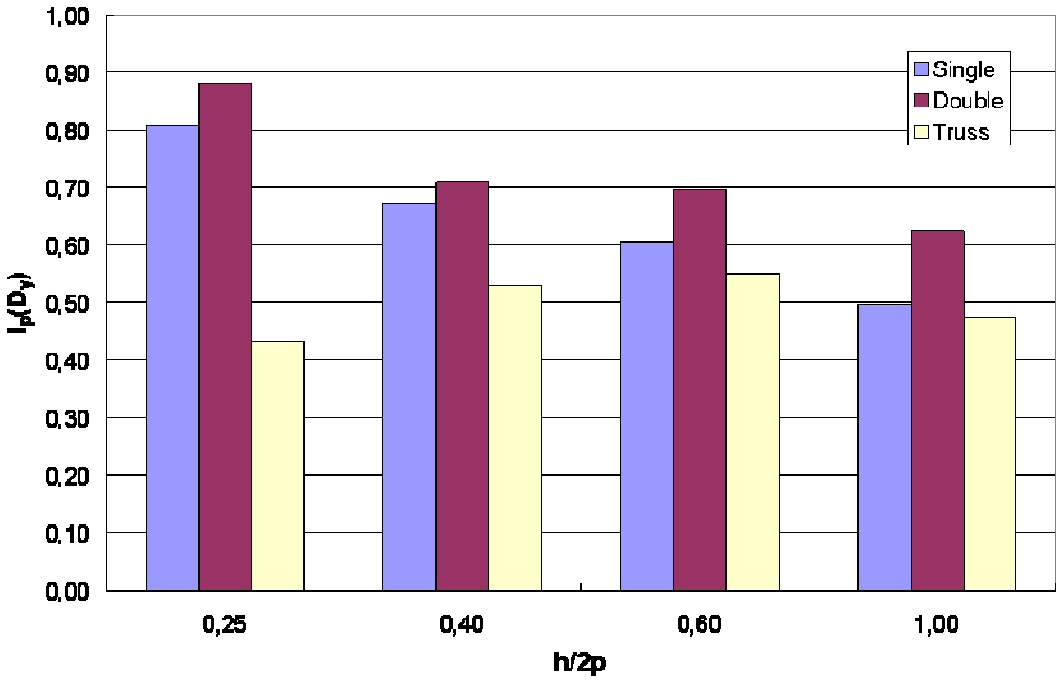

Figure 10. Performance of the sandwich configurations with respect to equivalent Dy.